Volume 7 | Number 41 | 7 November 2019 | Pages 6259–6460

Journal of Materials Chemistry B

Materials for biology and medicine

rsc.li/materials-b

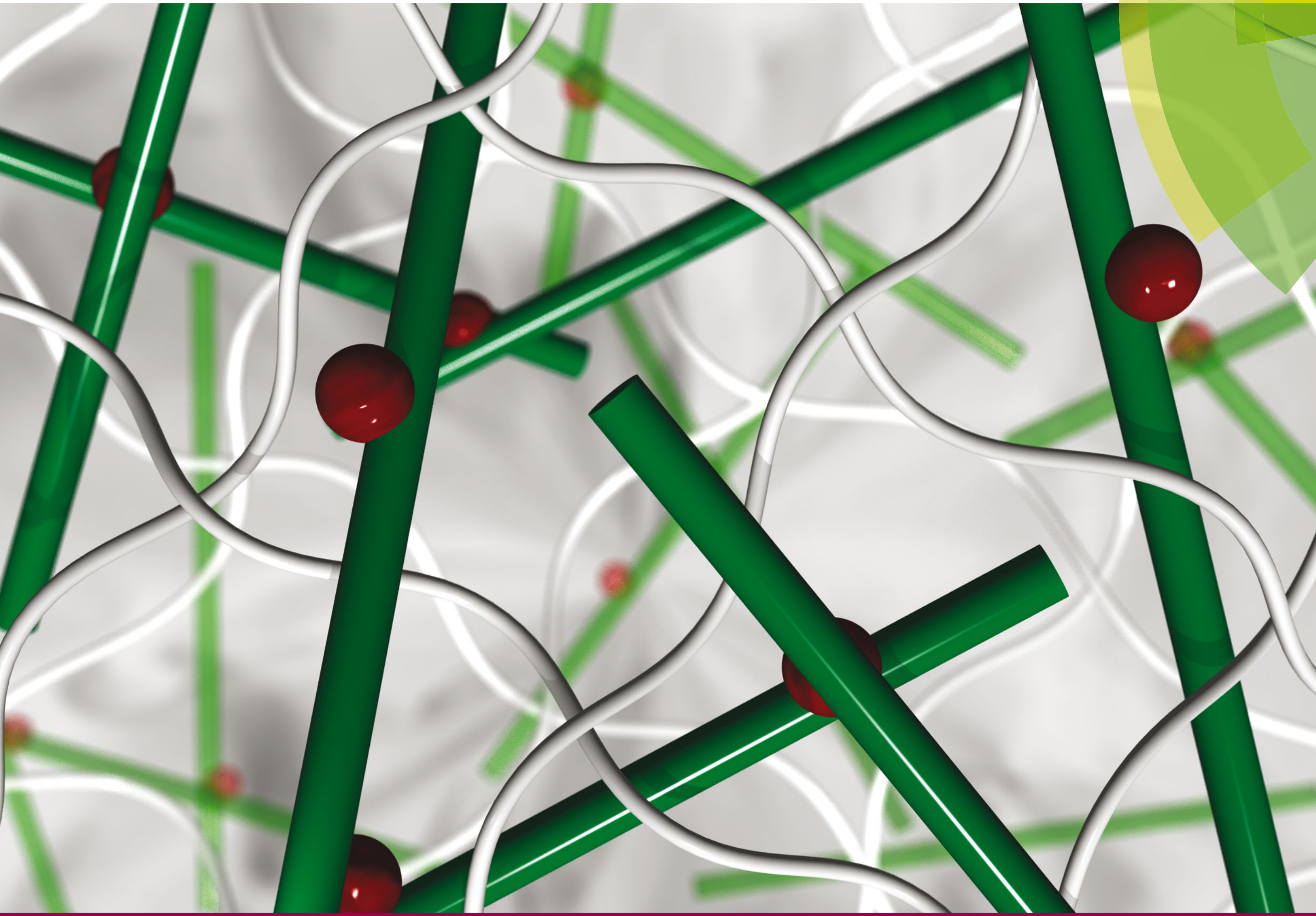

Themed issue: Emerging Investigators 2019

ISSN 2050-750X

ROYAL SOCIETY OF CHEMISTRY | Celebrating IYPT 2019

COMMUNICATION
Daniel R. King, Jian Ping Gong *et al.*
Double network hydrogels based on semi-rigid polyelectrolyte physical networks

Journal of
Materials Chemistry B

COMMUNICATION

View Article Online
View Journal | View Issue

Check for updates

Cite this: *J. Mater. Chem. B*, 2019, 7, 6347

Received 18th June 2019,
Accepted 10th July 2019

DOI: 10.1039/c9tb01217f

rsc.li/materials-b

Double network hydrogels based on semi-rigid polyelectrolyte physical networks†

Riku Takahashi, ‡§[a] Takuma Ikai,§[a] Takayuki Kurokawa, [bc] Daniel R. King *[bc] and Jian Ping Gong *[bcd]

Applying the double network principle to develop tough hydrogels with different polymer chemistries is important for the potential application of hydrogel materials. Synthesis of the two interpenetrated networks with contrasting structure and properties required for double networks usually involves a two-step polymerization process. In this work, we present a new method to synthesize tough double network hydrogels by post-physical crosslinking of linear semi-rigid polyelectrolytes entrapped in a chemically crosslinked neutral network. Owing to their semi-rigid structure, the linear polyelectrolytes form a brittle physical network above their overlap concentration in multi-valent $ZrCl_2O$ ion solutions without macroscopic phase separation within the flexible neutral network. The double network hydrogels thus prepared exhibit high modulus (∼1.7 MPa), strength (∼1.3 MPa), fracture strain (∼7.3), and strain energy density (∼5.9 MJ m^{-3}), while containing over 80% water. These materials also exhibit modest self-healing ability (∼51% after 30 minutes), demonstrating an additional benefit of a physical sacrificial network. This method is simpler than the conventional two-step polymerization and could be applied to develop tough hydrogels from rigid polyelectrolytes, including biopolymers such as DNA, HA, and chondroitin sulfate.

Introduction

Hydrogels, a class of soft/wet materials, exhibit unique properties that cannot be found in hard/dry materials, including low friction,[1] high biocompatibility,[2] and high permeability.[3] Conventional hydrogels are brittle and fragile however, limiting their applications. The brittleness of hydrogels originates from heterogeneity in the network structure and high solvent content.[4,5] The former induces stress concentration locally during deformation, and the latter causes low resistance against crack propagation. To overcome such limitations, intense efforts have focused on developing mechanisms to increase the mechanical properties of hydrogels. Breakthroughs have occurred owing to the development of the following techniques: (1) suppressing crack initiation by homogenization of the network structure (*e.g.* slide-ring gels and Tetra-PEG gels),[6,7] and (2) preventing crack propagation by stress yielding (nanocomposite gels and double network (DN) gels).[8,9] Among them, DN gels, consisting of an interpenetrating brittle/hard network and stretchable/soft network, exhibit noteworthy properties including high Young's modulus (∼10^5–10^6 Pa) and tremendous toughness (∼4500 J m^{-2}) despite containing high (∼90%) water content.[10,11] Therefore, DN gels have great potential for applications in biomedical fields that required stiffness, toughness, and biocompatibility.[12,13]

The profound toughness of DN gels is due to the "sacrificial bond principle",[11] where energy is dissipated by fracture of the brittle/hard network prior to rupture of the stretchable/soft network. Conventionally, we synthesize a chemically crosslinked polyelectrolyte network as the sacrificial network. Polyelectrolytes are chosen because they exhibit a high swelling ratio in pure water. When soaked in a monomer solution of the second stretchable/soft network, the crosslinked polyelectrolyte network extends, taking up large quantities of solution even with a relatively high crosslinking density, which is subsequently polymerized. This results in a double network gel consisting of a highly extended polyelectrolyte first network at low concentrations interpenetrated with a dense and stretchable second network. Due to this fabrication process, a two-step polymerization is necessary to obtain typical DN gels with contrasting interpenetrated network structure, requiring much time and effort. Additionally, since the first network is chemically crosslinked,

---

[a] *Graduate School of Life Science, Hokkaido University, Sapporo 001-0021, Japan*
[b] *Faculty of Advanced Life Science, Hokkaido University, Sapporo 001-0021, Japan. E-mail: dking@sci.hokudai.ac.jp, gong@sci.hokudai.ac.jp*
[c] *Global Station for Soft Matter, Global Institution for Collaborative Research and Education (GI-CoRE), Hokkaido University, Japan*
[d] *Institute for Chemical Reaction Design and Discovery (WPI-ICReDD), Hokkaido University, Sapporo, 001-0021, Japan*

† Electronic supplementary information (ESI) available: Additional experimental details. See DOI: 10.1039/c9tb01217f

‡ Current Address: NTT Basic Research Laboratories, NTT Corporation, 3-1 Morinosato-Wakamiya, Atsugi, Kanagawa, 243-0198, Japan.

§ The authors contributed equally to this work.

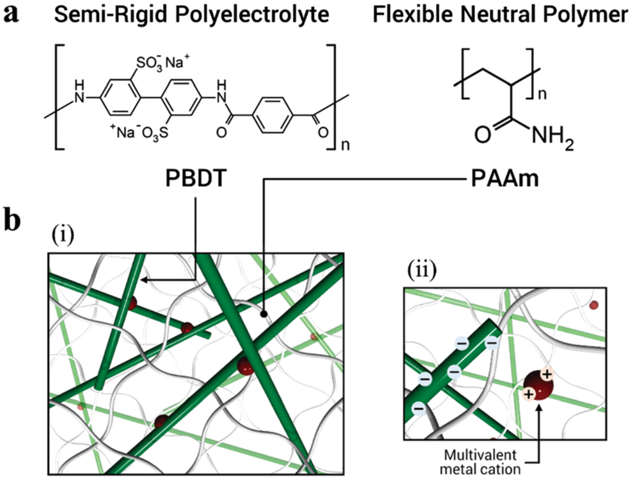

Fig. 1 Fabrication concept for one-pot DN hydrogels utilizing a semi-rigid polymer-based physical sacrificial network. (a) Chemical structures of the semi-rigid polyelectrolyte, PBDT, and flexible neutral polymer, polyacrylamide (PAAm). (b) (i) Schematic illustration of the semi-rigid polymer network formed inside the stretchable polymer network *via* immersion in multi-valent ion solutions. The persistence length of PBDT is ∼100 times greater than PAAm, and therefore is depicted as rod-like for illustration purposes. (ii) Crosslinking of the sacrificial network occurs by physical bonding between the negatively charged PBDT and positively charged ions. The green chains, grey chains and red spheres represent the PBDT, PAAm and multi-valent ions, respectively.

it is not capable of exhibiting self-healing properties. Therefore, finding new methods to create sacrificial networks is a great challenge for not only improving the simplicity of the conventional method but also obtaining outstanding soft materials for use in aqueous environments with enhanced mechanical properties.

To achieve these goals, we designed a technique to fabricate physical/chemical DN hydrogels through a ''one-pot'' polymerization, based on post-ion crosslinking of linear rigid polyelectrolytes entrapped in a chemically crosslinked neutral network (Fig. 1). We choose intrinsically rigid polyelectrolytes because (1) the rigid rod structure greatly contrasts the flexible neutral polymer, which should improve the stiffness of the composite gel, (2) the high persistence length should allow for overlap to occur at small concentrations, and (3) the rigid structure prevents collapse into a condensed phase in high ionic strength environments, which occurs for flexible polyelectrolytes.

To demonstrate this idea, we combined the semi-rigid polyelectrolyte, poly(2,2′-disulfonyl-4,4′-benzidine terephthalamide) (PBDT) and a chemically crosslinked polyacrylamide network. PBDT has a long persistence length of ∼40 nm to give a small overlap concentration ($C^* \sim 0.3$ wt%).[14] PBDT is water soluble, and has found use in applications ranging from viscosity modifiers to gel electrolytes.[15–17] PBDT and other polyelectrolytes have shown the ability to form a hard/brittle physically crosslinked network by ion complexation with multi-valent ions.[18–21] To synthesis the DN gels by a one-pot process, this polyelectrolyte is added to a precursor solution containing acrylamide and a chemical crosslinker, and subsequently a PAAm chemically crosslinked gel containing linear PBDT molecules is polymerized. After that, the PBDT-containing PAAm gel is immersed in multi-valent ion solution to form a physical network of PBDT. By this physical gel formation, PBDT/PAAm DN gels consisting of a brittle/hard sacrificial PBDT network and the stretchable polyacrylamide network is formed. Notably, the formation of the sacrificial physical network occurs after the synthesis of the stretchable network, in contrast to traditional DN gels. Unique properties including high dissipation and modest self-healing of the sacrificial network were observed. We found that the multivalent $ZrCl_2O$ ions act as a unique crosslinker for the formation of the physical PBDT network, which forms above the overlap concentration of PBDT. The method introduced here enables the fabrication of physical/chemical DN hydrogels through a simple one-pot polymerization, with robust mechanical properties and modest self-healing abilities. This method may be applicable for fabricating DN gels from rigid polymers including biopolymers such as DNA, HA, and chitosan.

Results and discussion

Characterization of PBDT/PAAm hydrogels

Initial characterization of the system was carried out on samples containing 3.0 M PAAm and 3 wt% PBDT in the as-prepared state. To verify the formation of the PBDT network inside the PAAm hydrogel matrix, we compared the swelling ratio (Q, equilibrium volume divided by the as-prepared volume) of PBDT/PAAm gels and neat PAAm gels in solutions containing various types of ions (0.15 M) (Fig. 2a and b). The neat PAAm gels showed almost the same swelling ratio (Q = 4–5), regardless of solution. On the other hand, the swelling ratio of the PBDT/PAAm gels were strongly related to the solution. Due to the high osmotic pressure of the polyelectrolyte, the PBDT/PAAm gels exhibited high swelling in pure water ($Q \sim 9.5$), which is known as the molecular stent effect.[22] In the NaCl solution, the swelling ratio of PBDT/PAAm gels is much lower than that in pure water but was still slightly higher than that of pure PAAm gels, indicating that the 0.15 M monovalent metal ions can somewhat suppress the osmotic pressure of the polyelectrolytes, but not completely. However, in the $CaCl_2$ and $AlCl_3$ solutions, the swelling ratios of the PBDT/PAAm gels were slightly less than that of the PAAm gels. When the PBDT/PAAm gels were immersed in the $ZrCl_2O$ solution, the swelling ratio decreased dramatically ($Q \sim 2$), likely due to the PBDT molecules forming a network structure as shown in Fig. 1b(i). $ZrCl_2O$ exists as a complex highly hydrated compound, $[Zr(OH)_2{\cdot}4H_2O]_4[Cl_8{\cdot}12H_2O]$, where the cation is an octavalent tetramer complex $[Zr(OH)_2{\cdot}4H_2O]_4^{8+}$.[23] We will refer to this structure as $ZrCl_2O$ for simplicity.

Physical network formation by ionic bonding was verified by attenuated total reflectance Fourier-transform infrared spectroscopy (ATR-FTIR, Fig. 2c). A 4 wt% solution of PBDT in water was prepared. This solution was dropped into 0.15 M solutions containing $CaCl_2$, $AlCl_3$, or $ZrCl_2O$. The resulting physical gel was then placed on the ATR crystal and analyzed. A characteristic peak for the S=O stretching of the sulfonate group was observed at 1187 cm^{-1} for the 4 wt% PBDT aqueous solutions in the un-crosslinked form. After immersing the 4 wt% PBDT solution

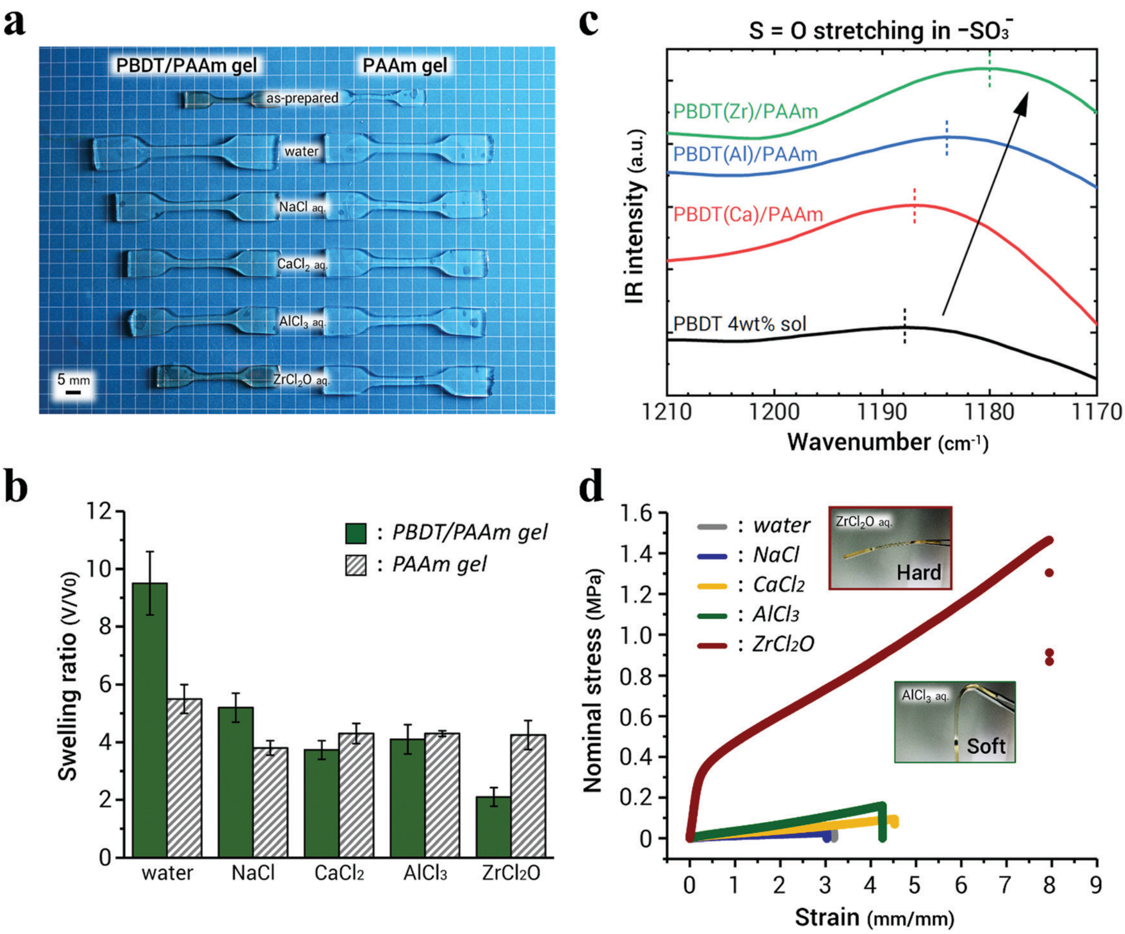

Fig. 2 Physical and mechanical properties of PBDT/PAAm gels. (a) Photographs of 3 wt% PBDT/PAAm and neat PAAm gels in the as-prepared state and swollen state in various ion solutions. (b) Swelling ratio of the gels after immersion in different ion solutions. (c) ATR-FTIR experiments were performed on PBDT physical gels with varying ion type. Gels were made containing 4 wt% PBDT and ionic concentration of 0.15 M. Peak shifts were compared to PBDT 4 wt% solutions in water. A vertical shift was applied to the data for clarity and (d) stress–strain curves of 3 wt% PBDT/PAAm gels formed in different ion solutions with ionic concentration of 0.15 M. Insets demonstrate the qualitative difference in strength between the $ZrCl_2O$ and $AlCl_3$ immersed samples.

into 0.15 M ion solutions, the sulfonate peak shifted to lower wavenumber with increasing valency of the ions. We hypothesize that the strongest network structures can form with $ZrCl_2O$ because the compound is octavalent (+8), meaning it can form many bonds with the sulfonate groups of PBDT. Since immersion in $ZrCl_2O$ solution causes the gel to exhibit the largest shift in the FTIR spectrum, we can infer that this gel has the highest concentration of physical bonds. This agrees with the swelling results. The decreased swelling ratio observed in PBDT/PAAm gels with high valency cations likely occurs because PBDT molecules can strongly bind and form physical networks in the PAAm matrix, suppressing osmotic swelling.

The formation of the PBDT network in the PAAm gel matrix caused a significant increase in mechanical properties, similar to the increase seen in traditional double network hydrogels. Fig. 2d shows typical tensile stress–strain curves of the 3 wt% PBDT/PAAm gels swollen in various 0.15 M solutions. The water-equilibrated PBDT/PAAm gel was soft and elastic with low Young's modulus of 14 ± 0.2 kPa, low fracture stress of 26 ± 3 kPa, and low fracture strain of 2.8 ± 0.4. No ions are present to crosslink the sacrificial network, and therefore it has no influence on the mechanical response of the gel. In the case of the NaCl solution-equilibrated sample, the gels exhibited similar mechanical properties to the water-swollen sample. Monovalent ions cannot act as a crosslinking agent, only forming associations with individual chains. The $CaCl_2$ and $AlCl_3$ solution-swollen samples were also soft and elastic; however, the mechanical properties did increase slightly with the increasing cationic nature of the ions (see Table S1 for details, ESI†), as some crosslinking can occur. When the PBDT/PAAm gels were immersed in $ZrCl_2O$ solution, a clear yielding behavior with high Young's modulus of 1.69 ± 0.02 MPa, high fracture stress of 1.34 ± 0.09 MPa, and high fracture strain of 7.29 ± 0.47 was observed. This dramatic increase in mechanical properties coincides well with the result of the swelling ratio of the PBDT/PAAm gels, which implies the formation of a sacrificial network.

Effect of $ZrCl_2O$ concentration on mechanical properties

As the cation valency increases, the number of associations that can occur also increases. Modifying the number of associations is analogous to changing the crosslink density of the first network in chemical DN gels, which is important towards DN gel mechanical characteristics.[24] In DN gels containing a physically crosslinked first network, ionic concentration also influences physical crosslinking density (Fig. 3). Fig. 3a contains stress–strain curves for 3 wt% PBDT/PAAm gels in varying concentration $ZrCl_2O$ solutions. Fig. 3b–d contain the Young's modulus, fracture strain, and fracture stress from these stress–strain curves, respectively. We see in general that mechanical properties exhibit a parabolic shape with increasing $ZrCl_2O$ concentration. At low concentrations, the gel is weaker and more fragile, exhibiting properties more closely related to the neat chemical gel, PAAm. A sufficient concentration, over 0.15 M, is required to maximize the number of crosslinking events; one $ZrCl_2O$ ion should form physical bonds with more than one PBDT chain. Concentration that is too high suppresses the probability for a multi-valent ion to form ionic bonding to multiple chains. If excess ions are added, above 0.5 M, the sulfonate groups on PBDT may become saturated, and not all cations of the $ZrCl_2O$ complex will bind with other PBDT molecules. If some $ZrCl_2O$ remains unbound, more swelling will occur and a weaker gel will result. We find that between 0.15 M and 0.50 M, the mechanical properties become optimized. This is clearly seen from the strain energy density, a measure of toughness calculated by integrating the area under the stress–strain curve, Fig. 3e. With a concentration of 0.3 M, the strain energy density reaches 7.6 ± 0.9 MJ m^{-3}. This value is comparable to the toughest double network and viscoelastic hybrid gels. By optimizing the ion type and concentration, very tough hydrogels can be fabricated based on a physical sacrificial network.

Healing ability

Many tough hydrogels have been fabricated that utilize ionic interactions as a healing mechanism.[25,26] When stress is released, elastic restoring force causes recovery of strain and ionic interactions can reform. In this system we observed partial self-recovery. Cyclic tests were performed by applying either low (ε = 0.5, Fig. 4a) or high (ε = 4, Fig. 4b) strains at a constant displacement rate, and then returning to zero strain at the same displacement rate. Recoverability was measured as a function of waiting times between cycles. During the first cycle of the virgin sample, significant hysteresis is observed. This is evidence of the destruction of the sacrificial network; an important property of DN gels is hysteresis during cycle testing. However, in contrast to DN gels, upon reloading the samples, for both low and high strains, some hysteresis is recovered. Hysteresis recovery as a function of waiting time is shown for low and high strain in Fig. 4c and d, respectively. In both cases, we see that as waiting time increases, healing efficiency increases. Maximum healing efficiencies were measured for low strain of 51.3% after 30 minutes, and for high strain of 23.8% after one hour. These results provide additional evidence that energy is dissipated through the physical sacrificial network *via* dynamic interactions.[27] The toughening mechanism of PBDT/PAAm gels shares many similarities with recently reported stiff and tough gels such as phase-separated PAAm gels[28] and tri-block copolymer DN gels,[29] where breaking physical bonds is the primary mechanism of energy dissipation. A significant benefit of utilizing physical bonds in the sacrificial network is their ability to heal after removing the applied deformation.

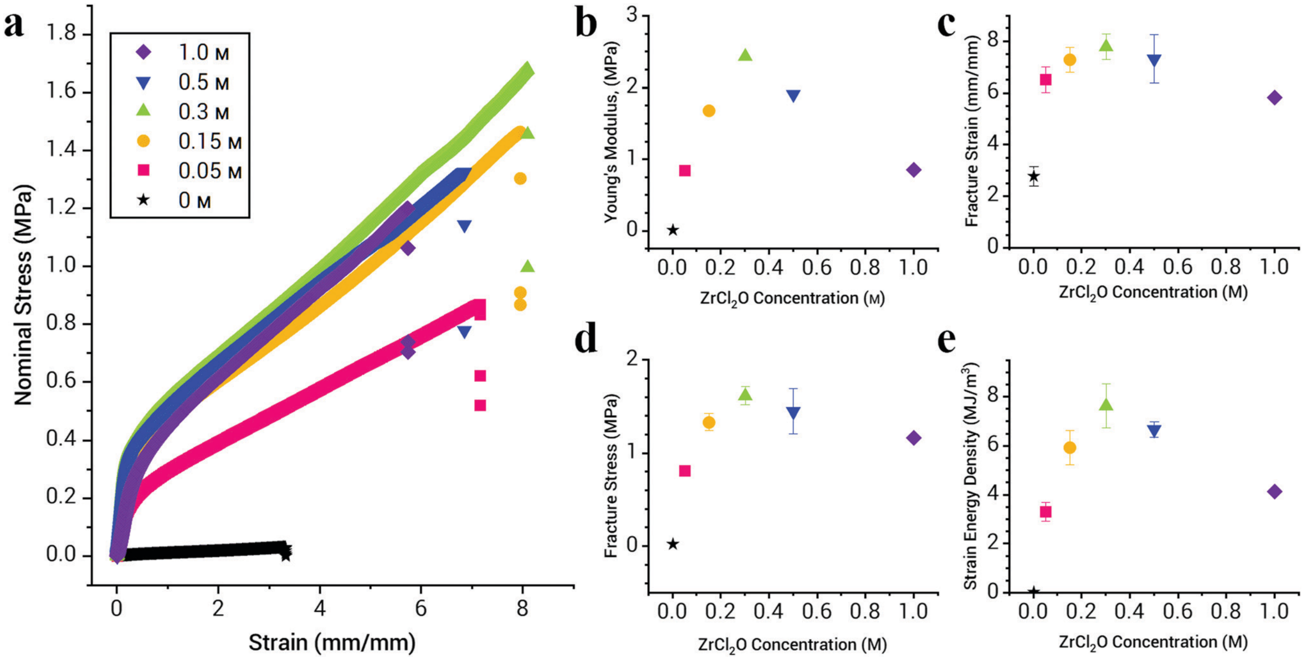

Fig. 3 Mechanical properties of the 3% PBDT/PAAm gels immersed in $ZrCl_2O$ solutions from 0 to 1 M. (a) Stress–strain curves. (b) Young's modulus. (c) Strain at break. (d) Stress at break. (e) Strain energy density. The error bars are standard deviation from the results of 3–5 samples and are present unless the error bars are smaller than the symbol size.

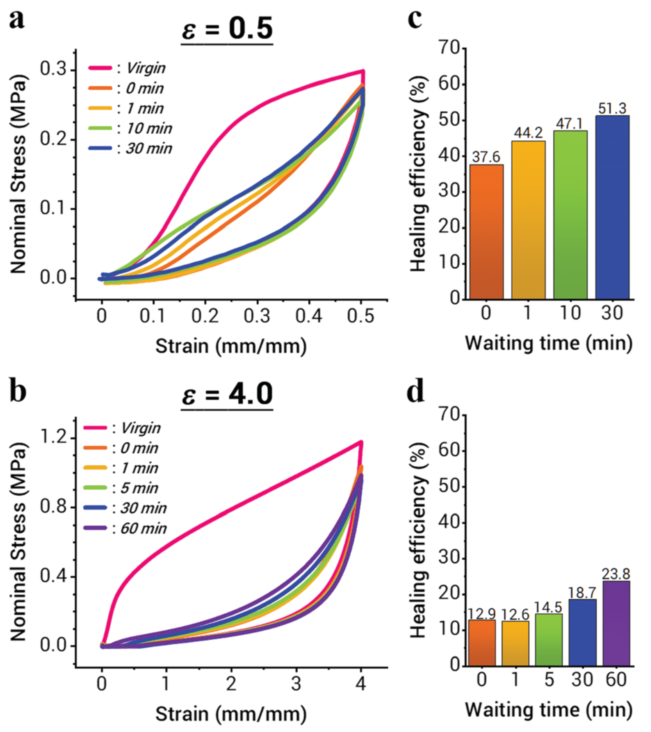

Fig. 4 Cyclic loading/unloading test of the 3% PBDT/PAAm gels after equilibration in 0.15 M $ZrCl_2O$ solution. Stress–strain curves for cycle testing at strains of (a) 0.5 or (b) 4.0 with different waiting times after testing. Healing efficiency at a maximum strain of (c) 0.5 and (d) 4.0 was estimated by comparing the mechanical hysteresis of the first cycle test to the cycle tests after various waiting times.

Effect of PBDT concentration on sacrificial network formation

To form a double network structure, the PBDT molecules must exist in sufficiently high concentrations to form a continuous network structure by ionic crosslinking. Next, we aim to elucidate the influence of PBDT concentration on the structure formation and resulting properties of the physical DN gel. As we saw in Fig. 2a, the presence of a sacrificial network resists swelling. Samples were prepared with varying PBDT concentration in 0.15 M $ZrCl_2O$ solution. Fig. 5a shows the swelling ratio of these gels, based on the as-prepared concentration, $C_{p,0}$, after immersion in the $ZrCl_2O$ solution. We see that all samples show swelling relative to the as-prepared state ($Q > 1$), which indicates that the equilibrium concentration of PBDT is lower than in the as-prepared state. The equilibrium concentration of PBDT, $C_{p,e}$ can be calculated by dividing $C_{p,0}$ by the swelling ratio, Q. By plotting $C_{p,e}$ *versus* $C_{p,0}$ in Fig. 5b, we are directly comparing the relationship between the PBDT concentration in the as-prepared state and the equilibrium state in these gels. Samples falling below the line representing a slope of 1 exhibit greater swelling in water, because the difference between as-prepared and equilibrium swelling is greater. As the PBDT concentration increases, the swelling ratio decreases (symbols fall closer to the line). From this we can infer that increased PBDT concentration results in a stronger sacrificial network.

To study the effect of PBDT concentration on the mechanical properties, we performed uniaxial tensile tests on the $ZrCl_2O$ solution-equilibrated PBDT/PAAm gels with different PBDT concentrations, Fig. 5c. The colors of the plotted stress–strain curves match with the concentrations plotted in Fig. 5a and b. When only a small amount of PBDT is present ($C_{p,0} = 0.1$ wt%), the sample exhibits properties similar to neat PAAm (plotted in black and almost entirely eclipsed). Increasing the PBDT content to $C_{p,0} = 1$ wt% causes an increase in modulus, but a linear stress–strain response is maintained. Further increasing to $C_{p,0} = 2$ wt% results in the introduction of a yielding point along with further increasing modulus. Young's modulus, yield stress, fracture strain and fracture stress continue to increase with increasing $C_{p,0}$ up to $C_{p,0} = 5$ wt%, which possesses extremely high Young's modulus of 5.04 ± 0.32 MPa, high fracture stress of 2.70 ± 0.13 MPa, and high fracture strain of 10.8 ± 0.15. The enhancement ratio ($C_{p,0} = 5$ wt% PBDT/neat PAAm) of Young's modulus and work of extension reached ~280 and ~110, respectively.

To understand what causes the transition to improved mechanical properties, Young's modulus is plotted both *versus* $C_{p,0}$ and $C_{p,e}$ in Fig. 5d. Two trends are clearly visible. At low concentration, the modulus increases slowly with increasing concentration, because PBDT acts merely as a filler and cannot form a network. At a critical concentration of $C_{p,0}^* \sim 0.8$ wt% based on the as-prepared state or $C_{p,e}^* \sim 0.3$ wt% for the equilibrium state, a notable change in slope occurs, and modulus increases at a much quicker rate. $C_{p,0}^*$ is much higher than the reported overlap concentration, C_{ref}^* (red band in Fig. 5d), while $C_{p,e}^*$ matches the literature value of $C_{ref}^* = 0.3$ wt%, for PBDT with comparable molecular weight ($M_w = 180$ kDa *versus* 142 kDa of this work).[14] This is reasonable since the ionic crosslinking occurs during the swelling process. For gels formed with $C_{p,0} = 0.6\%$, in the as-prepared state the PBDT will overlap, but upon immersion in salt solution swelling occurs, resulting in $C_{p,e} = 0.2\%$, and therefore a network structure cannot form. This sample exhibits low Young's modulus and does not undergo yielding. When the concentration of PBDT satisfies both overlap and possesses multi-valent crosslinking, a network forms that significantly increases the mechanical strength and toughness of the composite. These results indicate that only a few wt% of semi-rigid polymers are required to significantly reinforced bulk hydrogels. Utilizing the sacrificial bond principle enabled highly effective enhancement of an ordinary hydrogel.

While hydrogels are generally clear, we noticed that large loadings of PBDT influenced the clarity of the samples. To quantify this change, we measured the transparency of the samples. The results are presented in Table S1 (ESI†). For the PAAm-ion samples, and for the PBDT/PAAm samples in water, the transparency was nearly 100%. However, we see in the case of PBDT/PAAm in $ZrCl_2O$ solution, as the PBDT concentration increases, the transparency decreases. When $C_{p,e} = 0.39$ wt%, or just greater than C_{ref}^*, transparency was 91%. Increasing to $C_{p,e} = 1.8$ wt% the transparency was 83%. Further increasing to $C_{p,e} = 3.8$ wt% and the transparency drops to 62%. PBDT of similar molecular weight was shown to exhibit a critical nematic liquid crystal concentration, $C_{LC}^* = 2.2$ wt%.[18] Ordering within the gel likely contributes to both the increased

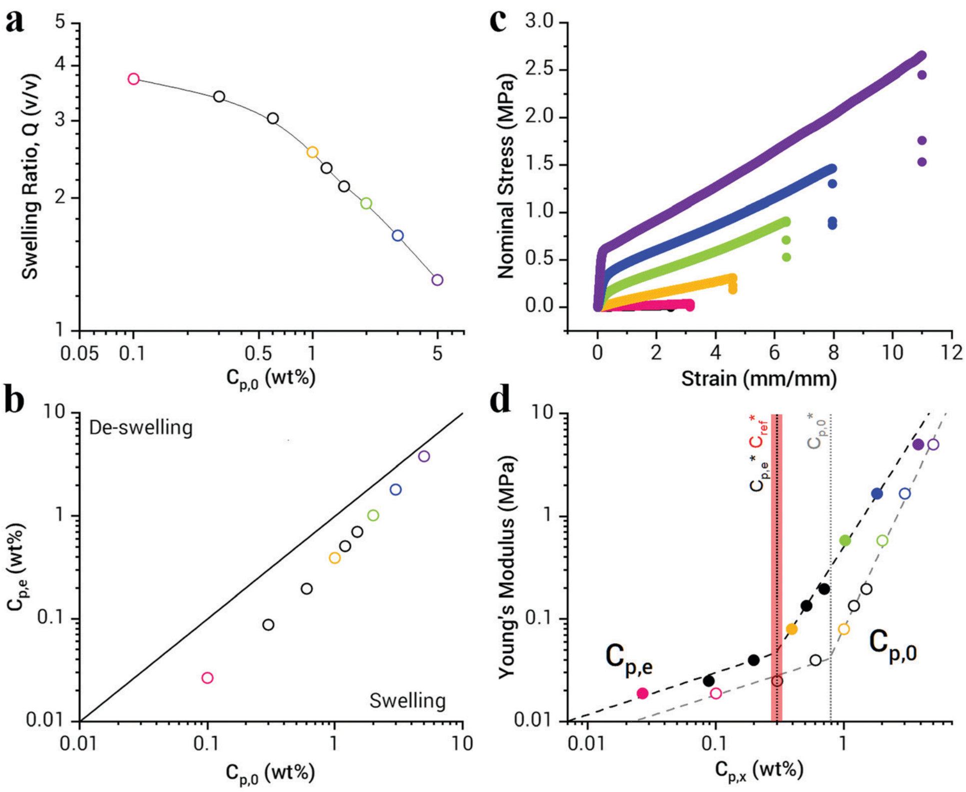

Fig. 5 Influence of PBDT concentration. (a) Swelling ratio *versus* as-prepared PBDT concentration. (b) A plot comparing equilibrium and as-prepared concentration, $C_{p,e}$ *versus* $C_{p,0}$, which demonstrates the relative swelling nature of each composition. As the PBDT concentration increases, swelling decreases. (c) Stress–strain curves of PBDT/PAAm gels with different concentrations of PBDT in the hydrogel matrix. Colors correspond with the concentrations from (a) and (b). (d) Relationship between Young's modulus of PBDT/PAAm gels and PBDT concentration, either $C_{p,0}$ or $C_{p,e}$. The symbols represent the average of 3–5 samples and in all cases error bars are smaller than the symbol size. Red vertical band represents the literature overlap concentration, C_{ref}* of PBDT. Vertical dotted black and gray lines represent the apparent critical concentrations of PBDT in either the equilibrium condition $C_{p,e}$* or as-prepared condition $C_{p,0}$*, respectively. Dashed trend lines are drawn as guides for the eye. All samples were equilibrated in 0.15 M $ZrCl_2O$ solution.

mechanical response as well as the decreased transparency. In general, the formation of a physical sacrificial network with PBDT by $ZrCl_2O$ crosslinking results in large aggregates that are capable of scattering light. As these aggregates become stronger, the tensile properties increase, but the larger aggregates also scatter more light, resulting in a decrease in transparency. Based on these results, optimum physical DN gels are formed when the $C_{p,e}$ is between 0.3 wt% and 2.2 wt%, allowing high mechanical performance and maintaining clarity.

Importance of chain rigidity

Polymer chain rigidity is an important factor for creating sacrificial networks based on polyelectrolytes. For a polyelectrolyte with an intrinsically flexible chain, the charged backbone of the polyelectrolyte extends in pure water but changes to a coiled conformation in ionic solutions and even collapses in multivalent ion solutions. We overcame this problem by using intrinsically rigid polyelectrolytes that can maintain their extended conformation even in high ionic strength environments. To test the importance of persistence length, we substituted PBDT with a relatively flexible polymer, poly(2-acrylamido-2-methyl propane sulfonic acid) sodium salt (PNaAMPS). In the presence of even small concentrations of salt, the persistence length of PNaAMPS is on the order of only a few nm.[30,31] The synthesized PNaAMPS had a M_w of 2830 kDa, M_n of 392 kDa, and a $Đ$ of 7.2. With such a large molecular weight, the 3 wt% PNaAMPS solution will be above the overlap concentration even in high ionic strength. After synthesizing a PAAm gel containing 3 wt% linear PNaAMPS, we immersed the PNaAMPS/PAAm gel in 0.15 M $ZrCl_2O$ solution, following the same method as for the PBDT/PAAm gels (see ESI† for details). After reaching the equilibrium state, we performed uniaxial tensile tests (Fig. S1, ESI†). The PNaAMPS/PAAm gel was soft and elastic with low Young's modulus of 29 ± 1.6 kPa, low fracture stress of 135 ± 20 kPa, and fracture strain of 4.52 ± 0.42, contrasting the results seen for the PBDT/PAAm gel. Due to its high molecular weight, the PNaAMPS is expected to overlap and form a network. However, this physical network could not serve as a sacrificial network, because the presence of ions prevents chain extension. Without an extended network, the PNaAMPS chains do not break preferentially during deformation, and therefore a double network structure is not formed. The PBDT structure we use is inherently rigid, allowing it to work well to form an extended chain sacrificial network, even in the presence of ions. These results demonstrate that the rigidity of the physical gel polymer plays an important role, matching the essence of the extended polyelectrolyte 1st network in conventional DN gel.[9]

Conclusion

The mechanical properties of semi-rigid PBDT/polyacrylamide composite hydrogels were significantly enhanced *via* swelling in $ZrCl_2O$ multi-valent ion solution. Toughening was induced by the creation of a stiff, physical sacrificial network; thus, the intensity of the cationic nature of the ions, the concentration of ions, the concentration of the semi-rigid polymers, and the rigidity of the polymer chains are all important parameters influencing the effectiveness of the sacrificial network. These networks possess partial self-healing ability. Along with these excellent properties, these hydrogels still contain 80% water. The strategy introduced here represents a useful method to create DN gels through ''one-pot'' polymerization and post-modification and should be generally applicable to systems beyond PBDT/PAAm, including other rigid/stretchable polymer system such as rigid biopolymers (*e.g.* DNA, microtubule, and collagen)[32] and flexible biopolymers (*e.g.* polysaccharides).[33] We believe that this method will find application as tunable soft materials for use in aqueous environments.

Experimental section

Preparation of PBDT/PAAm hydrogels

To synthesize the hydrogel films, reaction cells were prepared by sandwiching a square framed silicone spacer (thickness: 1 mm) between two parallel glass plates. The aqueous pre-gel solutions contained 3.0 M of the neutral monomer, AAm, 0–5.0 wt% of the semi-rigid anionic polymer, PBDT (M_w = 142 kDa; M_n = 110 kDa; $Đ$ = 1.29), 0.1 mol% of the chemical crosslinker, *N*,*N*′-methylenebisacrylamide (MBAA), and 0.5 mol% of the thermal-initiator, potassium persulfate (KPS) (mol% is relative to the monomer). Additional information about synthesis of PBDT can be found in the ESI.† After proper mixing, the pre-gel solution was poured into the reaction cell. Thermal-induced free radical polymerization was carried out in air in a temperature-controlled heat box (60 °C) for 10 h. After thermal polymerization, the as-prepared sheet-like gels (about $60 \times 60 \times 1.0$ mm^3) were carefully removed from the reaction cells.

Swelling in various solutions containing multi-valent ions

The as-prepared PBDT/PAAm gels were immersed in a large amount of pure water or different multi-valent ion solutions (NaCl, $CaCl_2$, $AlCl_3$, $ZrCl_2O$) for 24 h, respectively. Unless otherwise stated, the concentration of the ionic solution was 0.15 M. Subsequently, the ion-loaded hydrogels were immersed in deionized water for 24 h to remove excess ions. The swelling ratio, Q, or volume-change relative to the as-prepared state, V/V_0, was calculated from the size change in the three dimensions.

Mechanical testing

Uniaxial tensile tests were performed on swollen samples using a tensile-compressive tester (Instron 5965 type universal testing system). Samples were cut into a dog-bone shape standardized as JIS-K6251-7 sizes (length 35 mm, width 6 mm, thickness 1.5–3, gauge length 12 mm, inner width 2 mm) with a gel cutting machine (Dumb Bell Co., Ltd). The fracture stress and fracture strain were defined as the nominal stress and strain at the breaking point, respectively. Young's modulus was defined as the initial slope of the stress–strain curves. Strain energy density was defined as the area under the stress–strain curve.

Cyclic loading/unloading tests

The cyclic loading/unloading tensile tests for evaluating the self-healing ability of the PBDT/PAAm gels swollen in $ZrCl_2O$ solution was performed on one sample repeatedly by using an Instron 5965 type universal testing system. The PBDT/PAAm gels were stretched to $\varepsilon = 0.5$ or 4 at a velocity of 100 mm min^{-1} at room temperature. Then, samples were returned to the initial displacement immediately at the same velocity as stretching. After each loading/unloading test, the samples were left to stand at room temperature for a prescribed time (1, 5, 30 or 60 min). During testing, the samples were covered with silicone oil to prevent drying. The energy dissipation was estimated from the hysteresis area, U_{hys} by:

$$U_{\mathrm{hys}} = \int_{\varepsilon=0}^{\varepsilon=4} (\sigma_{\mathrm{load}} - \sigma_{\mathrm{unload}})\mathrm{d}\varepsilon$$

where σ_{load} and σ_{unload} are the stress during loading and unloading, respectively. From the U_{hys} of the virgin sample compared to subsequent tests after various waiting times, the healing efficiency (%) was calculated.

Conflicts of interest

There are no conflicts to declare.

Acknowledgements

This research was financially supported by Grant-in-Aid for Scientific Research (No. 17H06144) and Grant-in-Aid for JSPS Fellows (No. 15J01078) from the Japan Society for the Promotion of Science (JSPS). R. T. was supported by MEXT through the Program for Leading Graduate Schools (Hokkaido University ''Ambitious Leader's Program''). Institute for Chemical Reaction Design and Discovery (ICReDD) was established by World Premier International Research Initiative (WPI), MEXT, Japan.

References

1 S. Ma, M. Scaraggi, D. Wang, X. Wang, Y. Liang, W. Liu, D. Dini and F. Zhou, *Adv. Funct. Mater.*, 2015, **25**, 7366–7374.
2 P. Li, Y. F. Poon, W. Li, H.-Y. Zhu, S. H. Yeap, Y. Cao, X. Qi, C. Zhou, M. Lamrani, R. W. Beuerman, E.-T. Kang, Y. Mu, C. M. Li, M. W. Chang, S. S. Jan Leong and M. B. Chan-Park, *Nat. Mater.*, 2011, **10**, 149–156.
3 M. C. Branco, D. J. Pochan, N. J. Wagner and J. P. Schneider, *Biomaterials*, 2010, **31**, 9527–9534.
4 M. Shibayama, *Bull. Chem. Soc. Jpn.*, 2006, **79**, 1799–1819.
5 K. S. Anseth, C. N. Bowman and L. Brannon-Peppas, *Biomaterials*, 1996, **17**, 1647–1657.
6 Y. Okumura and K. Ito, *Adv. Mater.*, 2001, **13**, 485–487.

7 N. Sasaki, T. Matsunaga, M. Shibayama, S. Suzuki, Y. Yamamoto, R. Yoshida, C. Ito, T. Sakai and U. Chung, *Macromolecules*, 2008, **41**, 5379–5384.

8 K. Haraguchi and T. Takehisa, *Adv. Mater.*, 2002, **14**, 1120.

9 J. P. Gong, Y. Katsuyama, T. Kurokawa and Y. Osada, *Adv. Mater.*, 2003, **15**, 1155–1158.

10 T. Nakajima, H. Furukawa, Y. Tanaka, T. Kurokawa, Y. Osada and J. P. Gong, *Macromolecules*, 2009, **42**, 2184–2189.

11 J. P. Gong, *Soft Matter*, 2010, **6**, 2583.

12 J. Saito, H. Furukawa, T. Kurokawa, R. Kuwabara, S. Kuroda, J. Hu, Y. Tanaka, J. P. Gong, N. Kitamura and K. Yasuda, *Polym. Chem.*, 2011, **2**, 575–580.

13 K. Yasuda, N. Kitamura, J. P. Gong, K. Arakaki, H. J. Kwon, S. Onodera, Y. M. Chen, T. Kurokawa, F. Kanaya, Y. Ohmiya and Y. Osada, *Macromol. Biosci.*, 2009, **9**, 307–316.

14 W. Yang, H. Furukawa, Y. Shigekura, K. Shikinaka, Y. Osada and J. P. Gong, *Macromolecules*, 2008, **41**, 1791–1799.

15 N. Sarkar and L. D. Kershner, *J. Appl. Polym. Sci.*, 1996, **62**, 393–408.

16 Y. Wang, J. Gao, T. J. Dingemans and L. A. Madsen, *Macromolecules*, 2014, **47**, 2984–2992.

17 Y. Wang, Y. Chen, J. Gao, H. G. Yoon, L. Jin, M. Forsyth, T. J. Dingemans and L. A. Madsen, *Adv. Mater.*, 2016, **28**, 2571–2578.

18 Z. L. Wu, T. Kurokawa, S. Liang, H. Furukawa and J. P. Gong, *J. Am. Chem. Soc.*, 2010, **132**, 10064–10069.

19 W. Yang, H. Furukawa and J. P. Gong, *Adv. Mater.*, 2008, **20**, 4499–4503.

20 Z. L. Wu, T. Kurokawa, D. Sawada, J. Hu, H. Furukawa and J. P. Gong, *Macromolecules*, 2011, **44**, 3535–3541.

21 C. H. Yang, M. X. Wang, H. Haider, J. H. Yang, J. Y. Sun, Y. M. Chen, J. Zhou and Z. Suo, *ACS Appl. Mater. Interfaces*, 2013, **5**, 10418–10422.

22 T. Nakajima, H. Sato, Y. Zhao, S. Kawahara, T. Kurokawa, K. Sugahara and J. P. Gong, *Adv. Funct. Mater.*, 2012, **22**, 4426–4432.

23 K. Matsui and M. Ohgai, *J. Am. Ceram. Soc.*, 2005, **80**, 1949–1956.

24 T. Matsuda, T. Nakajima, Y. Fukuda, W. Hong, T. Sakai, T. Kurokawa, U. Il Chung and J. P. Gong, *Macromolecules*, 2016, **49**, 1865–1872.

25 J.-Y. Sun, X. Zhao, W. R. K. Illeperuma, O. Chaudhuri, K. H. Oh, D. J. Mooney, J. J. Vlassak and Z. Suo, *Nature*, 2012, **489**, 133–136.

26 T. L. Sun, T. Kurokawa, S. Kuroda, A. Bin Ihsan, T. Akasaki, K. Sato, M. A. Haque, T. Nakajima and J. P. Gong, *Nat. Mater.*, 2013, **12**, 932–937.

27 P. Lin, S. Ma, X. Wang and F. Zhou, *Adv. Mater.*, 2015, **27**, 2054–2059.

28 K. Sato, T. Nakajima, T. Hisamatsu, T. Nonoyama, T. Kurokawa and J. P. Gong, *Adv. Mater.*, 2015, **27**, 6990–6998.

29 H. J. Zhang, T. L. Sun, A. K. Zhang, Y. Ikura, T. Nakajima, T. Nonoyama, T. Kurokawa, O. Ito, H. Ishitobi and J. P. Gong, *Adv. Mater.*, 2016, **28**, 4884–4890.

30 M. Tricot, *Macromolecules*, 1984, **17**, 1698–1704.

31 T. Hattori, S. Bat-Aldar, R. Kato, H. B. Bohidar and P. L. Dubin, *Anal. Biochem.*, 2005, **342**, 229–236.

32 P. A. Janmey, D. R. Slochower, Y. H. Wang, Q. Wen and A. Cebers, *Soft Matter*, 2014, **10**, 1439–1449.

33 R. L. Cleland, *Arch. Biochem. Biophys.*, 1977, **180**, 57–68.